Perception, 2000, volume 29, pages 581 – 600

DOI:10.1068/p3043

Role of chromaticity, contrast, and local orientation cues in the perception of density

William H A Beaudot, Kathy T Mullen
McGill Vision Research, Department of Ophthalmology, McGill University, 687 Pine Avenue West (H4-14), Montreal, Quebec H3A 1A1, Canada; e-mail: wbeaudot@vision.mcgill.ca
Received 14 July 1999, in revised form 21 January 2000

Abstract. We compared the role of the red – green, blue – yellow, and luminance post-receptoral mechanisms in the perception of density. The task requires the comparison of densities between two stimuli composed of oriented bandpass elements, pseudo-randomly scattered across an area of constant size. The perception of density differences was measured by a temporal 2AFC procedure for all pairs of mechanisms and for four possible densities. We found that stimuli of identical physical densities are not perceived equally: there is a consistent bias in favour of blue – yellow stimuli which are perceived as significantly more dense than red – green and achromatic stimuli. We considered three factors that could have differentially affected the density perception of blue – yellow stimuli: an increase in the perceived size of the individual blue – yellow elements, a perceived contrast difference, and the presence of local orientation cues. We found that the increased perceived density of the blue – yellow stimuli occurred despite the fact that there was no increase in perceived size of the individual elements, and remained despite corrections for the two other factors. We conclude that the significant increase in perceived density for the blue – yellow mechanism is a global effect, associated with a perceived colour 'melting' of the elements in the array. Our data were fitted with the occupancy model of Allik and Tuulmets (1991, *Perception & Psychophysics* **49** 303 – 314) and we found that blue – yellow stimuli have a greater 'occupancy' than red – green or achromatic stimuli.

1 Introduction

Among the many features characterising the organisation of the visual scene, the spatial distribution of its elements plays an important role. The perception of density, or numerosity, reflects one aspect of this spatial distribution, indicating proximity between neighbouring elements irrespective of their individual properties. Density has been investigated as a key attribute of pre-attentive textural processing; texture discrimination clearly depends on both the spacing as well as the form of its elements, although the spacing must fall below a certain limit before elements cohere to generate the percept of a texture (Ellemberg et al 1998; Julesz 1981, 1986; Nothdurft 1985, 1990; Sagi and Julesz 1987; Wilkinson and Wilson 1998). Density is also an aspect of textural variation that can be used to determine shape and surface structure, although opinions on its importance in this role vary (Buckley et al 1996; Cumming et al 1993; Gibson 1950, 1979; Nawrot et al 1996; Stevens 1981). The importance of density in texture segregation is emphasised by the observation that the ability to segregate textures on the basis of element density and size develops very early in infancy, and before segmentation based on other regional differences such as orientation (Atkinson and Braddick 1992; Sireteanu and Rieth 1992). On the basis of observations of adaptations to texture density, it has been also suggested that density has its own neural representation, separable from those for correlated image properties such as spatial frequency (Durgin and Huk 1997).

Density perception is a global task, requiring the integration of information over a wide stimulus area, and is potentially dependent on a range of different factors. Previous studies have predominantly focused on the role of the spatial configuration of the stimulus. These have shown that the perception of density or numerosity is affected by the regularity of the arrangement of the pattern elements (Binet 1890, see Pollack and Brenner 1969; Alam et al 1986; Burgess and Barlow 1983; Ginsburg 1976, 1978, 1980;

Taves 1941), by the presence of clusterings of elements in the pattern (Allik and Tuulmets 1991; Ginsburg 1991; Ginsburg and Goldstein 1987), and by the element size and the area over which they are distributed (Allik et al 1991; Bindman and Chubbs 1998; Binet 1890; Ginsburg and Nicholls 1988; Krueger 1972).

To our knowledge, no study has looked specifically at the role of colour in the perception of density. A number of very early studies, however, examined how colour differences support figure–ground organisation and contour perception, and these reveal substantial differences between the two chromatic mechanisms, and between the chromatic and achromatic ones. In the following excerpt, Koffka (1936) describes the Liebmann effect for an isoluminous blue figure on a neutral ground: " ... a vague and vacillating blotch is seen, and even that may disappear completely for short periods of time. Therefore difference of stimulation between an enclosing and an enclosed area, if it is a mere colour difference, has, to say the least, much less power to produce a segregation of these two areas ... than a very small difference in luminosity" (page 126). It appears that the loss of form that characterises the Liebmann effect is much greater for the blue–yellow post-receptoral system than for the red–green one (Koffka and Harrower 1931; Tansley and Boynton 1978). Direct ratings of border distinctness also show that, while the red–green mechanism supports border perception with only a moderate loss of distinctness compared to the achromatic mechanism, the two sides of a blue–yellow border melt together yielding border ratings close to zero (Tansley and Boynton 1976, 1978). These observations have led to the suggestion that the primary function of the blue–yellow system is to signal chromaticity, whereas the red–green system supports both chromaticity and form (Boynton 1979).

Although interesting, these studies have only dealt with the perception of single chromatic borders and shapes, rather than how colour contrast is used in tasks requiring the integration of arrays of elements across space. Following this approach, a recent study on contour integration shows that the blue–yellow mechanism has no special deficiency in linking spatial information across element orientation and position to extract a contour (Mullen et al 2000), thus contradicting the idea that it is a purely chromatic system. Although we know that red–green chromatic contrast can support texture segregation (McIlhagga et al 1990), little is yet known about the role of the blue–yellow system in texture-based tasks.

The primary aim of this study has been to investigate the role of colour contrast in density perception. In pursuit of this aim we have also explored the effects of the perceived size of the elements, the element contrast, the distribution of elements across the visual field, and the influence of spatial structure within the stimulus. We used 'cardinal' stimuli that selectively isolate the responses of the three post-receptoral mechanisms (red–green, blue–yellow, and achromatic) in order to examine density perception by each alone. These three mechanisms differ from each other in a number of ways, including their contrast-sensitivity functions and spatial resolutions, absolute sensitivities to cone contrast, and their distributions across the visual field. A proper comparison of density perception by the three mechanisms requires that these differences be taken into account.

Previous studies of density perception have used dot stimuli which have a broad spatial-frequency spectrum. In the present study, we used spatial narrow-band stimuli (Gabor patches) in order to restrict the spatial-frequency content of the stimuli. This control has a number of advantages: it ensures that the measured contrast detection thresholds are always specific to one spatial frequency and cannot shift according to which spatial frequency is most easily detected by the visual field location of the particular post-receptoral mechanism under investigation. Furthermore, we selected a relatively low spatial frequency for the Gabor elements in order to reduce the impact of chromatic aberration (Bradley et al 1992).

Although the term 'numerosity' is also commonly used in the literature, we refer here to 'density' perception. We are confident that for our stimuli, with very large element arrays and a fixed stimulus area, the perceptions of 'density' and 'numerosity' correspond to the same visual 'impression', indicating that both terms reflect the same underlying process. However, asking subjects to judge numerosity would imply that some form of 'counting' is required, and also requires an assessment of the stimulus area in addition to the element density. Thus we think that density perception is a more direct assessment of the visual percept arising from the stimulus, and the term was readily understood by our subjects. As we have used a fixed stimulus area, which is not generally the case in other studies, density and numerosity correspond and the choice of terminology has no direct impact on our study.

2 Methods

2.1 *Stimuli*

The stimuli were square patches of pseudo-randomly distributed Gabor elements whose density could be varied (figure 1). The Gabor elements were odd symmetric and defined by the equation:

$$g(x, y, \theta) = c \sin[2\pi f(x \sin\theta + y \cos\theta)] \exp\left(-\frac{x^2 + y^2}{2\sigma^2}\right),$$

where θ is the element orientation in degrees, (x, y) is the distance in degrees from the element centre, c is the contrast, and σ is the space constant (0.17 deg). The peak frequency (f) was 1.5 cycles deg^{-1}, low enough to reduce luminance artifacts arising from chromatic aberration.

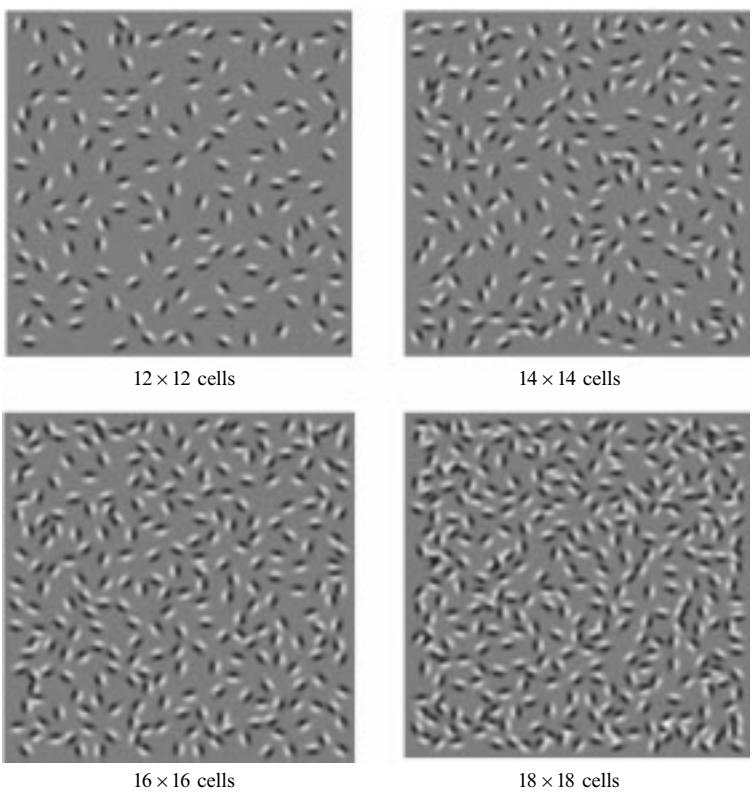

Figure 1. Examples of stimuli for the four densities used in the experiments.

A pseudo-random placement was used to prevent clumping and overlap of the elements. The stimulus area was divided up into a grid of invisible square cells and the centre of one Gabor element was placed randomly within each cell. If two elements in neighbouring cells overlapped, one Gabor was removed, producing an empty cell. No more than 8 empty cells were permitted per display and the average number was 4.

We used four different densities of the Gabor elements in the stimulus. The overall stimulus size was held constant, and the number of invisible cells per stimulus side was set to 12, 14, 16, or 18, giving a total of 144, 196, 256, and 324 cells in the stimulus. Depending on the density (0.7, 1.0, 1.3, or 1.6 elements deg^{-2}) the average distance between neighbouring Gabor elements was 1.4, 1.2, 1.0, or 0.9 deg. These interelement spacings are just above the 'texture-coherence limit' measured by Wilkinson and Wilson (1998), so that the element arrays are still perceived as separate elements and not as texture. The stimulus was viewed at 60 cm, and subtended a constant area of 504×504 pixels (14 deg $\times$ 14 deg). The stimulus was displayed in the centre of the screen subtending 27 deg $\times$ 22 deg.

2.2 *Chromatic properties*

The chromatic properties of the stimuli were defined within a three-dimensional cone contrast space. In this space, each axis represents the quantal catch of the L, M, and S cone types normalised with respect to the white background. Red–green, blue–yellow, and luminance cardinal stimuli were determined within this space. A cardinal stimulus isolates one post-receptoral mechanism and is invisible to the other two. We selected our cardinal stimuli from the knowledge of the cone weights of the three post-receptoral mechanisms provided by earlier studies (Cole et al 1993; Sankeralli and Mullen 1996). These studies have identified the relative cone weights of the mechanisms to be $L - M$ (the red–green mechanism), $S - \frac{1}{2}(L + M)$ (the blue–yellow mechanism), and approximately $x \cdot L + M$ (the luminance mechanism) where $x > 1$ and is variable between subjects. Within a cone contrast space, the cardinal direction is defined as the unique direction orthogonal to the vector directions representing the other two mechanisms. From the cone weights given above, the achromatic (Ach) cardinal direction is $L + M + S$ and the blue–yellow (BY) cardinal direction is the S-cone axis. The wide intersubject variability found for the luminance mechanism affects the specification of the red–green (RG) cardinal direction. Red–green isoluminance was determined for each subject individually by a motion-nulling technique (Anstis and Cavanagh 1983) for a patch of grating (1.5 cycles deg^{-1}, 3.6 deg^2) viewed binocularly and foveally and having the same mean luminance and chromaticity as the Gabor stimuli used in the main experiment.

2.3 *Apparatus and calibrations*

Stimuli were displayed on a Sony Trinitron 17 inch monitor with a Sun Sparcstation 2 computer. The monitor was driven by 8-bit D/A converters on a 24-bit frame-buffer. The spectral emissions of the red, green, and blue guns of the monitor were calibrated at the National Research Council of Canada with a Photo Research PR-700-PC SpectraScan. The monitor was gamma corrected in software with lookup tables based on luminance measurements obtained from a United Detector Technology Optometer (UDT S370) fitted with a 265 photometric sensor. The Smith and Pokorny fundamentals (Smith and Pokorny 1975) were used for the spectral absorption of the L, M, and S cones. From these data, a linear transform was calculated to specify the phosphor contrasts required for given cone contrasts (Cole and Hine 1992). The monitor was viewed in a blacked-out room, and the mean luminance of the display was 14.2 cd m^{-2}.

2.4 *Protocol*

A 2AFC task was used to measure the subject's ability to perceive a difference in density between two stimuli. Each trial consisted of a pair of stimuli presented sequentially for 0.5 s each. Presentations were abrupt with a 0.5 s interstimulus interval. The density of the stimulus in each pair was randomly selected from the four available. After each trial, the subject indicated the interval that contained the stimulus with the higher perceived density by pressing the appropriate mouse button. The experiment was continued until all 16 pairings of the four possible densities had been presented n times. The number of trials per condition (n) used for each experiment was between 9 and 20, and is given in the figure legends. No feedback was given. A black fixation mark appeared in the centre of the stimulus during each presentation. Stimuli were generated on-line, and a new stimulus was generated for each presentation.

In separate experiments, perceived densities were measured for different combinations of the three cardinal stimuli, giving six possible comparisons: three across different cardinal stimuli (RG with BY, RG with Ach, Ach with BY), and three within the same cardinal stimuli (RG with RG, etc). The combinations of the cardinal stimuli were tested in a balanced design. Practice trials were run before the experiment commenced.

2.5 *Observers*

The observers were two naïve volunteers (JM and JL), one non-naïve subject (AR), and the two authors (WB and KTM). All five had normal or refracted-to-normal vision, and all had normal colour vision according to the Farnsworth – Munsell 100-Hue Test. All experiments were done under binocular conditions.

3 Results

3.1 *The effect of colour on density perception*

Prior to exploring the effect of chromaticity on density perception, we matched the three cardinal stimuli (RG, BY, and Ach) in terms of their perceived contrast. This match was made in order to take into account the overall cone contrast sensitivity differences between the different post-receptoral mechanisms, but is complicated by the distributed nature of our stimuli and the differential losses in contrast sensitivity that occur across the visual field for the three mechanisms. For example, simply matching single Gabor elements in the fovea in threshold multiples is not successful at equating the perceived contrast of the three cardinal stimuli used for the density measurements (shown in figure 1) because red – green contrast sensitivity peaks sharply at the fovea, whereas blue – yellow and achromatic contrast sensitivities have a more even distribution (Mullen 1991; Mullen and Kingdom 1996; Mullen et al 2000). A perceived contrast match was made by a pairwise method of adjustment: two different cardinal stimuli were viewed consecutively and one was adjusted by the subject to match the other in overall perceived contrast. This was repeated until the subject was satisfied with the contrast match between the three cardinal stimuli.

For each possible density of one cardinal stimulus, we collected the proportion of responses for it being judged as denser than the comparison stimulus. Thus a proportion close to 0.5 means that the two stimuli are perceived as equally dense, while a value inferior or superior to 0.5 means that this stimulus is perceived as less or more dense, respectively, than the comparison. As explained in the protocol, four possible densities of the comparison stimulus were used, each presented n times. So as to derive a level of perceptual equivalence (the density at which the second stimulus is perceived as equal to the first), these data were fitted with a sigmoid-shaped function (a Weibull) given by:

$$P(x) = 1 - \exp[-(x/\alpha)^{\beta}],$$

where x denotes the density, and α and β the Weibull parameters.

Density of perceptual equivalence, D_{PE}, was defined as the density for which $P(x) = 0.5$, that is:

$$D_{PE} = \alpha \cdot (\ln 2)^{1/\beta}.$$

D_{PE} was extracted for each pair of stimuli, and was plotted as a contour of perceptual isodensity for each possible comparison between the cardinal stimuli. In this

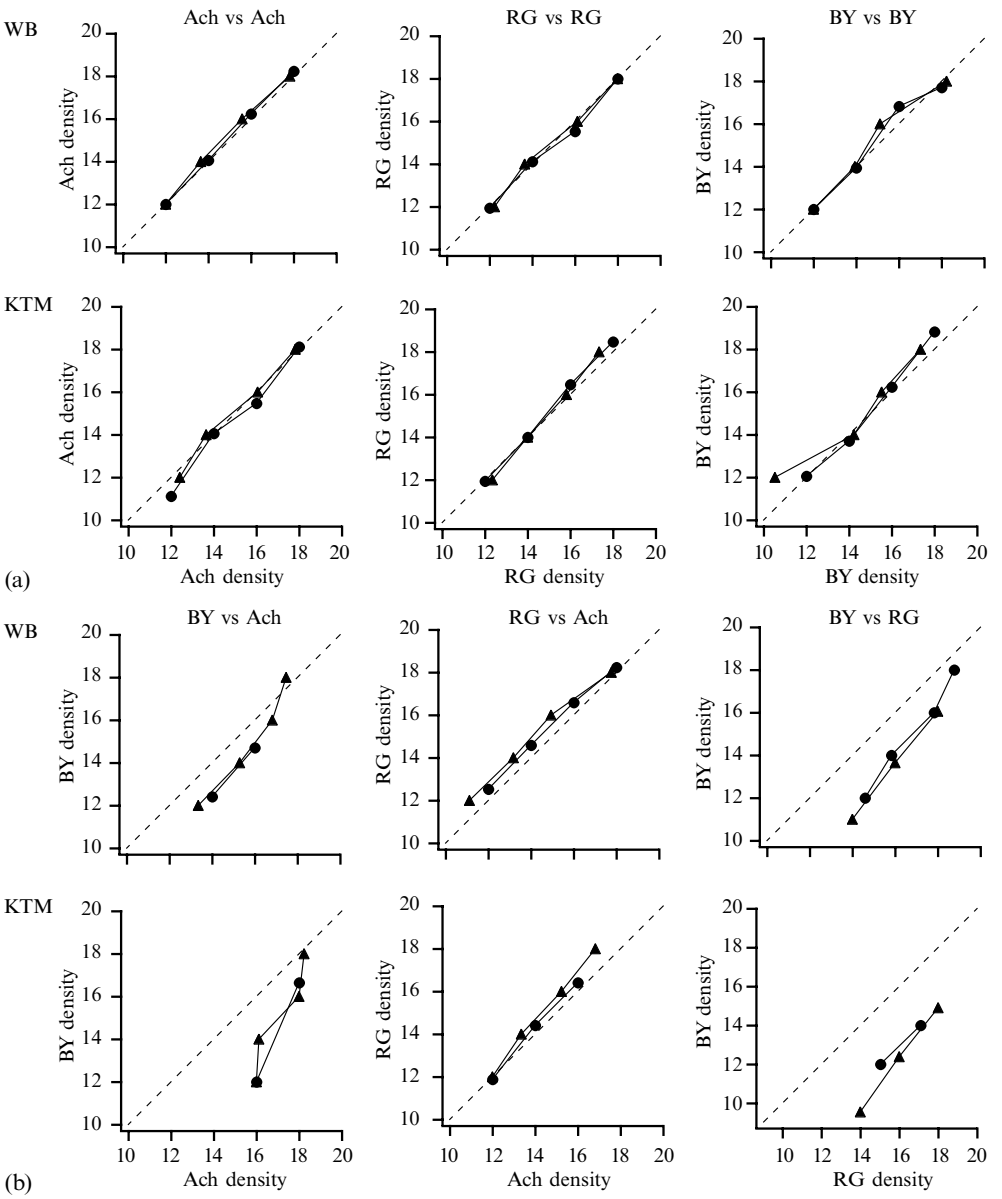

Figure 2. Perceptual density equivalence for two subjects (WB and KTM) (a) Perceptual equivalence for the within-mechanism conditions (Ach versus Ach, RG versus RG, BY versus BY). (b) Perceptual equivalence for the cross-mechanism conditions (BY versus Ach, RG versus Ach, BY versus RG). Data points lying below the dashed line indicate that stimuli from the *y*-axis are perceived as denser than stimuli from the *x*-axis. The unit for the density axis is the square root of the number of elements covering the stimulus field. Physical equivalence is represented by the diagonal dashed line. Circle and triangle data points represent the two sets of Weibull parameters extracted from the data fit. WB performed 20 trials per condition, and KTM performed 15.

representation, physical equivalence of density corresponds to the diagonal (dashed in the figures) line, while any deviation of the distribution of the data points from this line will indicate a bias in the perception of density in favour of one or other stimulus.

Figures 2 and 3 show the results for the five subjects; in all figures the dashed line represents the contour of physical isodensity, while the filled symbols represent data. Two sets of parameters were extracted from the data analysis, representing fits of one stimulus compared against different densities of the other stimulus, and vice versa, and are represented by triangle and circle symbols, respectively. The two sets of parameters are close to each other and reflect the stability of the parameter extraction. Figure 2a shows results of an initial control condition in which both cardinal stimuli were the same. This control was repeated for all subjects, but data are shown only for subjects WB and KTM. As expected, results show that perceptual equivalence matches physical equivalence when the two cardinal stimuli are the same. This control shows that the four chosen densities are distinguished without ambiguity, and so constitute a good range of distinguishable densities for all mechanisms.

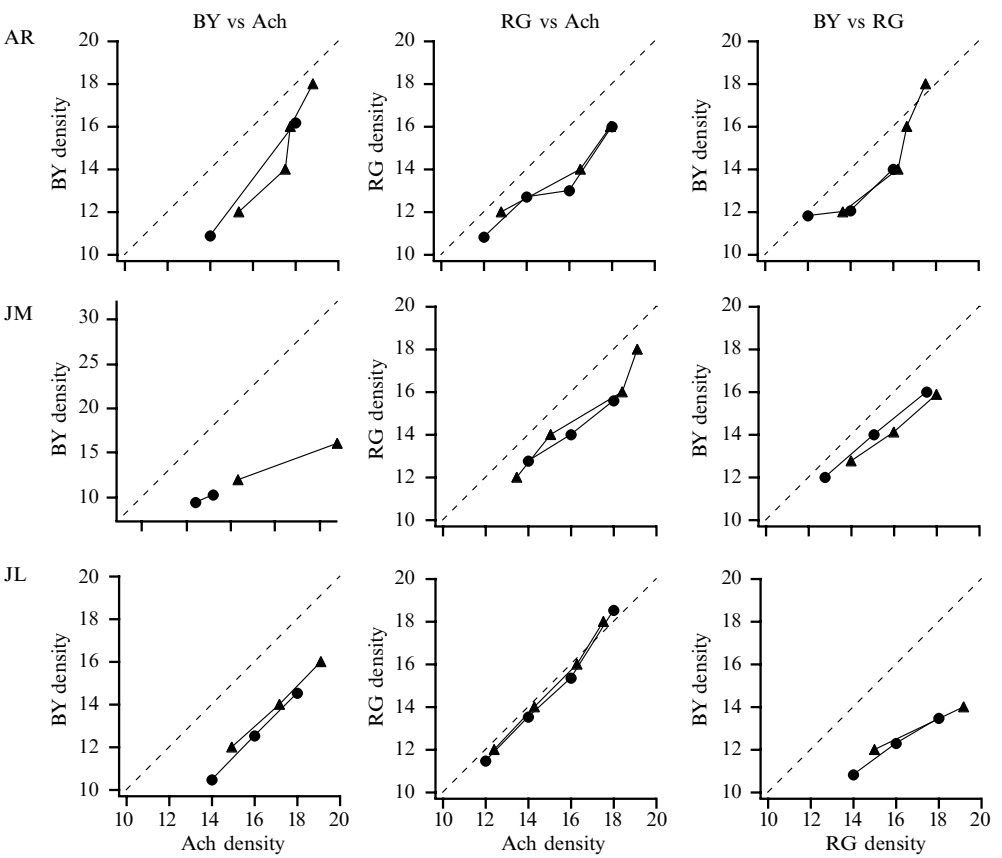

Figure 3. Perceptual density equivalence for the cross-mechanism conditions for three other subjects (perceptual equivalencies for the within-mechanism conditions are similar to those of subjects WB and KTM). Symbols and dashed lines are as for figure 2. All subjects performed 9 trials per condition.

Figures 2b and 3 show comparisons between different cardinal stimuli. Results are consistent across subjects and express a general trend of the data; the data points are displaced away from the line of physical equivalence (dashed line) indicating a shift in density perception. The data points are also more or less confined along a straight line, suggesting a linear dependence of the shift with density. The main result occurs

in the left and right panels and shows clearly that for all subjects there is a significant bias in favour of BY stimuli appearing denser when compared with the Ach or RG stimuli. The RG versus Ach comparison (middle panels) shows much less effect and is more variable across subjects: RG stimuli appear more dense than Ach stimuli for two subjects (AR and JM), and as dense as Ach stimuli for the three other subjects (WB, KTM, and JL).

To quantify these effects, we fitted a straight line (slope of 1) to the data with a horizontal shift parallel to the physical-density equivalence, and we extracted the horizontal shift of this line for each pair of mechanisms. Figure 4 shows this density shift for all conditions. All subjects show a strong bias in perception of density in favour of the blue–yellow stimuli compared with both achromatic and red–green stimuli: BY stimuli are perceived as consistently more dense than RG and Ach stimuli despite their physical equivalence. The average shift in density units of the BY mechanism among subjects is -3.8 and -2.4 relatively to the Ach and RG mechanisms, respectively. As mentioned above, the sign of the density bias between the red–green and achromatic stimuli is not systematic across subjects and the average bias across subjects is only -0.5. However, it is important to note that for every subject, the order in density perception is consistent across mechanisms, that is the density shift for Ach vs BY stimuli is roughly equal to the sum of the shift for Ach vs RG and that for RG vs BY stimuli. To support these conclusions, we analysed the significance of these effects using a 2-way ANOVA test with a Tukey–Kramer a posteriori analysis. This analysis shows that: (i) BY stimuli have a significantly greater perceived density ($p < 0.05$) in both BY/Ach and BY/RG conditions; and (ii) there is no significant difference across subjects, except for subject JM who shows a stronger perceived density for the BY stimulus than the other subjects.

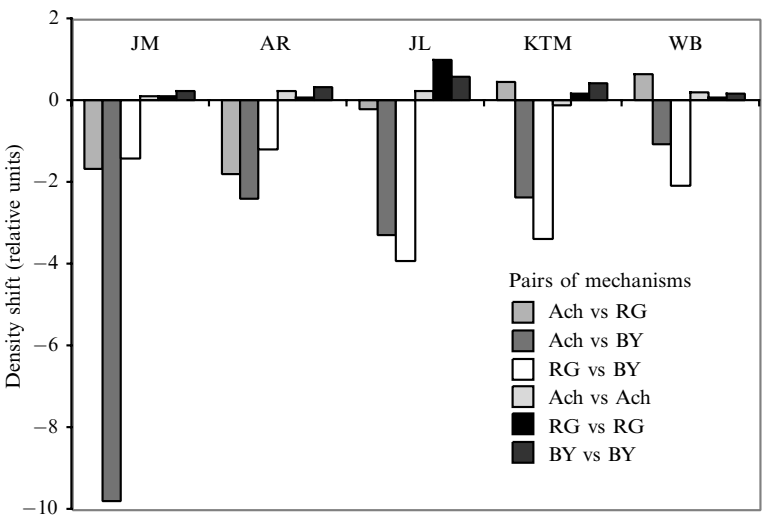

Figure 4. The horizontal shift (density shift) of the straight line fitted to the data of figures 2 and 3 parallel to the physical equivalence line (diagonal line) for each subject. The first three bars for each subject represent the shift in the cross-mechanism conditions. The last three bars represent the shift in the within-mechanism conditions (figures not shown in figure 3). A 2-way ANOVA test with a Tukey–Kramer a posteriori analysis indicates that the higher perceived density for the BY stimuli is significant ($p < 0.05$).

3.2 *Perceived size of individual elements*

We first consider whether an increase in the perceived size of individual blue–yellow elements could account for the increase in perceived density of these stimuli. We tested this hypothesis by perceptually matching the size of single Gabor element between the different chromatic mechanisms: Ach versus BY, RG versus BY, and Ach versus RG.

We used a temporal 2AFC staircase procedure in which one interval contained a Gabor element of constant size (the same as used in the density experiment) and the other interval contained a Gabor element of varying size from a different chromatic mechanism. The physical change in element size followed an inverse relationship between peak frequency and space constant of the Gabor element. The subject had to indicate which interval contained the larger Gabor element, and the size-varying element was then reduced or enlarged according to the subject's response to determine a perceived size match between the two elements. We performed this control experiment at a range of eccentricities (0–4 deg).

Results are shown in figure 5, in which the ratio of the perceived sizes of the Gabor elements is plotted as a function of eccentricity for the three mechanism pairs. The experiment was performed at two contrast levels: the contrast levels used in the original density-matching experiment (figures 2–4), and a contrast set in multiples of detection threshold for the individual Gabor elements determined for each eccentricity tested (2 × detection threshold for WB and 3 × detection threshold for KTM). Results show that the perceived size ratio remains at unity in all conditions, demonstrating that individual blue–yellow Gabor elements do not appear bigger than achromatic or red–green Gabor elements. This precludes any simple explanation of our density results based on a difference in perceived size between the individual stimulus elements.

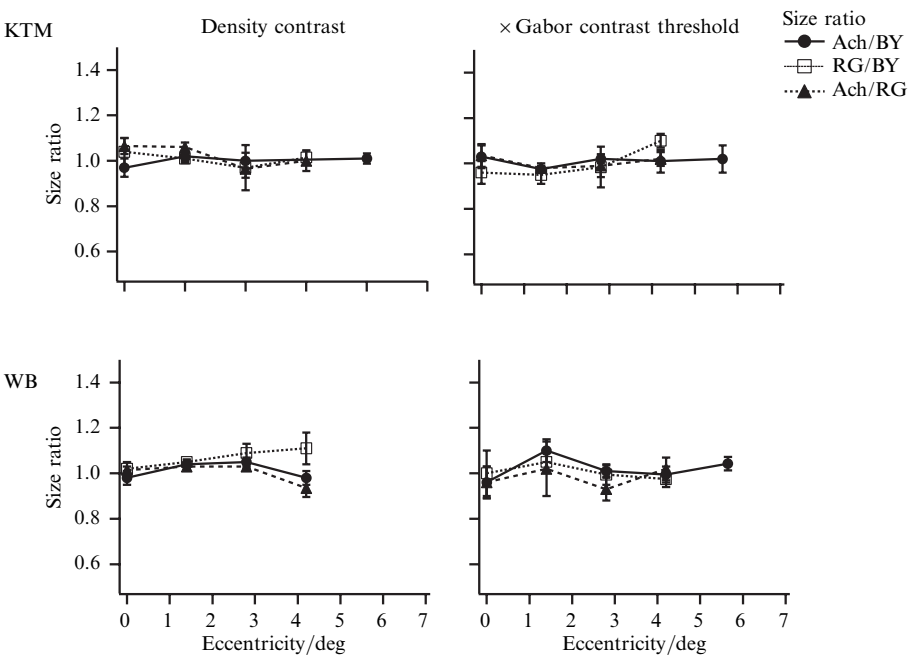

Figure 5. Size matching of single Gabor elements. The ratio of the perceived size of the Gabor elements is plotted as a function of eccentricity for both subjects and for the two contrast conditions. In each figure, every mechanism pair (C1/C2) is compared. A size ratio greater than unity means that stimulus C1 appears larger than C2. Each data point shows the average of 5 and 6 matches per condition for subjects WB and KTM, respectively. Error bars denote ±1 SD.

3.3 *Influence of contrast, eccentricity, and local structure on perceived density*

In this second group of experiments, we investigated three other possible factors that may influence the perception of density: specifically, the effects of contrast, eccentricity, and the presence of local structure within the stimuli.

3.3.1 *Effect of contrast.* From the ideal-observer point of view, the perception of density requires the assessment of the mean distance between neighbouring elements across space, and hence should be independent of the properties of the single elements. However it is quite sensible to propose that contrast or total luminance energy of the elements may affect the perceived density of those elements. For example, Mulligan and MacLeod (1988) have shown that element brightness and perceived dot density are related: an increase in dot density make dots appear brighter, suggesting that brightness is integrated over a distance of about 30 min of arc in radius. Our own informal observations also suggested that the perceived density of the stimulus may be influenced by the contrast of the individual elements, in that high-contrast elements tend to make the overall stimulus look 'richer' and denser in comparison to stimuli composed of low-contrast elements. On the other hand, an increase in contrast could reduce the uncertainty in density estimation without affecting perception of relative density per se; for example, high contrasts might decrease the positional uncertainty of the element centres, thus providing a more reliable estimate of the mean centre-to-centre distance and consequently of density.

Thus we investigated the possibility that contrast has a global effect on perceived density. We used a model in which the total contrast energy summed across the stimulus area is one possible measure of density by the visual system. In the following experiment, we tested for both a contrast effect and the viability of the contrast-energy model by measuring the effect of contrast on density perception and comparing the results with calculations of the contrast energy in the stimuli.

The contrast energy of the stimulus is defined by:

$$\sum_{1}^{n^2} C^2,$$

where C is contrast. The effect of contrast on perceived density was measured for pairs of the same cardinal stimuli (figure 6). Two different contrasts, each presented at four densities, were used (see legend). This was repeated for the three cardinal stimuli. If contrast fails to affect density perception, we expect the data to fall along the diagonal dashed line. The results for two subjects show that, for the three post-receptoral mechanisms, the data fall only slightly below this line, indicating a small bias favouring stimuli with the higher contrast as perceptually denser. This bias for the stimuli with the higher contrast also increases slightly with the density. However, a model based on calculating the stimulus energy alone predicts a much larger bias when intervals are equated in energy (thin line in figure 6). Thus, the data show that this hypothesis is not verified for any of the three mechanisms, suggesting that the subjects rely more on the physical density of the elements than on a global assessment of the stimulus contrast energy.

However, it is known that the red–green mechanism shows a steep decline in contrast sensitivity away from the fovea, whereas the other two mechanisms have a more constant contrast-sensitivity distribution across the stimulus field (Mullen 1991; Mullen and Kingdom 1996; Mullen et al 2000). Since we do not know which, if any, stimulus regions are the most relevant to the perception of density, we cannot predict whether this differential loss in red–green contrast sensitivity across the stimulus field has any effect on perceived density. However, the relatively steep loss in contrast that occurs away from the central region might reduce the overall perception of density in these stimuli, although it could not account for the differences on perceived density between the BY vs Ach stimuli since these have very similar contrast sensitivities across the visual field. In a further control experiment we tested this effect by modulating the overall contrast of the blue–yellow stimulus across the display so as to match the eccentricity-dependent modulation of the red–green stimulus. Blue–yellow contrast was attenuated

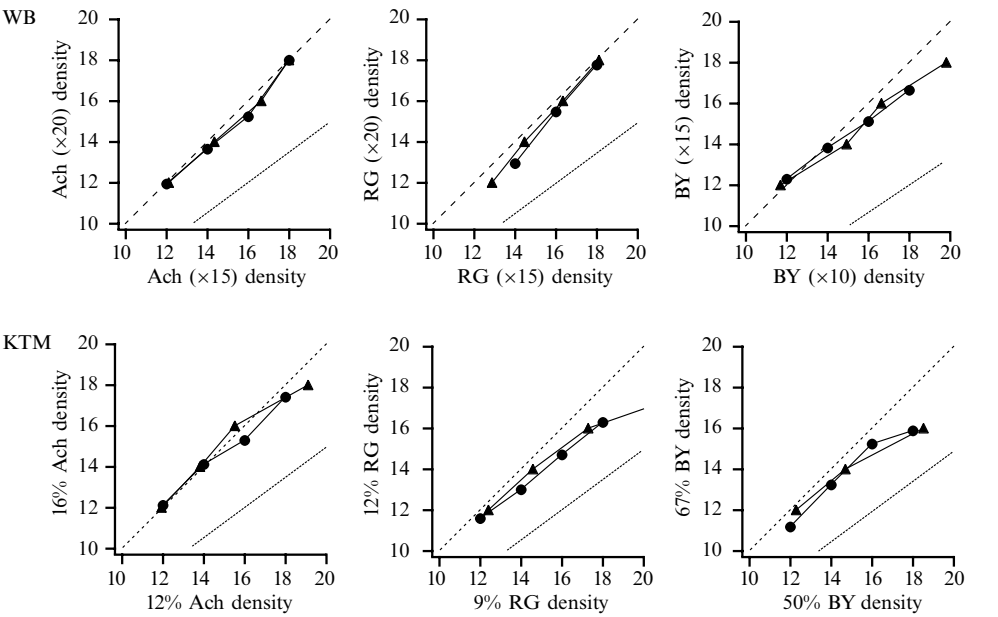

Figure 6. Effect of contrast on density perception. Data points in the three sets of graphs show perceptual density equivalence for each post-receptoral mechanism when the two members of a stimulus pair differ in contrast (expressed as multiple of contrast threshold for WB and absolute cone contrast for KTM). The vertical axis refers to the higher-contrast stimulus as marked, while the horizontal axis refers to the lower-contrast stimulus. Symbols and dashed lines are as for figure 2. The thin line represents the prediction of the contrast-energy hypothesis for density perception. 15 and 20 trials per condition for subjects KTM and WB, respectively.

across the stimulus field with a Gaussian function and was matched to the attenuation perceived for the red – green stimulus by a method of adjustment to vary the spread of the BY attenuation function. We find that the blue – yellow stimulus is still perceived as significantly denser than the physically equivalent red – green stimulus, showing that the steeper loss in RG contrast sensitivity with eccentricity compared to BY contrast sensitivity does not account for the increase in perceived density for the BY stimuli.

3.3.2 *Effect of local structure (curvature)*

We also looked at the effect of local structure on density perception. Since density perception has to rely on proximity between elements, any configuration involving local interaction between neighbouring elements (eg linking of co-oriented and collinear elements) is potentially able to bias the perception of density. This could be a critical feature for dense BY stimuli since neighbouring BY elements are perceived by all subjects as fusing among themselves. The proximity and the presence of local lines and curvatures could modify the salience of elements by, for example, enhancing their apparent contrast, or promoting some spreading effects. To test this hypothesis, we optimised the construction of stimuli so as to minimise the formation of local cues derived from local curvature and alignment of neighbouring elements. Previous work has shown that phase differences between nearby elements disrupt formation of local curvature (Field et al 2000; McIlhagga and Mullen 1996; Mullen et al 2000; Williams and Hess 1998). We used this property to minimise the formation of local curvature by reversing the polarity of elements so as to maximise a randomness criterion, formally equivalent to the minimisation of an edge relatability criterion as defined by Kellman and Shipley (1991). This randomness criterion, defined as the sum among each element neighbourhood of the difference between the direction made by this element and each of its neighbours and their respective orientations, minimises the in-phase collinearity of the

Gabor elements. Whatever the density, this procedure increases the randomness criterion by 20% over the whole stimulus.

We examined how the randomness in the stimulus affects density perception of the BY mechanism. BY stimuli were optimally randomised and their perceived density compared with RG and Ach stimuli. In figure 7, the $*$ symbol denotes the optimally randomised BY stimuli. In the cross-mechanism conditions (BY* vs Ach and BY* vs RG—left and middle panels in figure 7) for both subjects, the use of optimised BY stimuli does not significantly reduce the perceptual bias in favour of the BY stimulus in comparison with the original experiment with non-optimised stimuli. However, in the BY* – BY condition (right panels in figure 7), subject WB shows a density bias towards the optimised stimulus for the two highest densities, whereas subject KTM shows no bias. The fact that neither subject shows a density shift in favour of the non-optimised stimulus relatively to the optimised stimulus in the cross-mechanism condition precludes any significant role of local curvature in the density bias that we report for the BY stimuli.

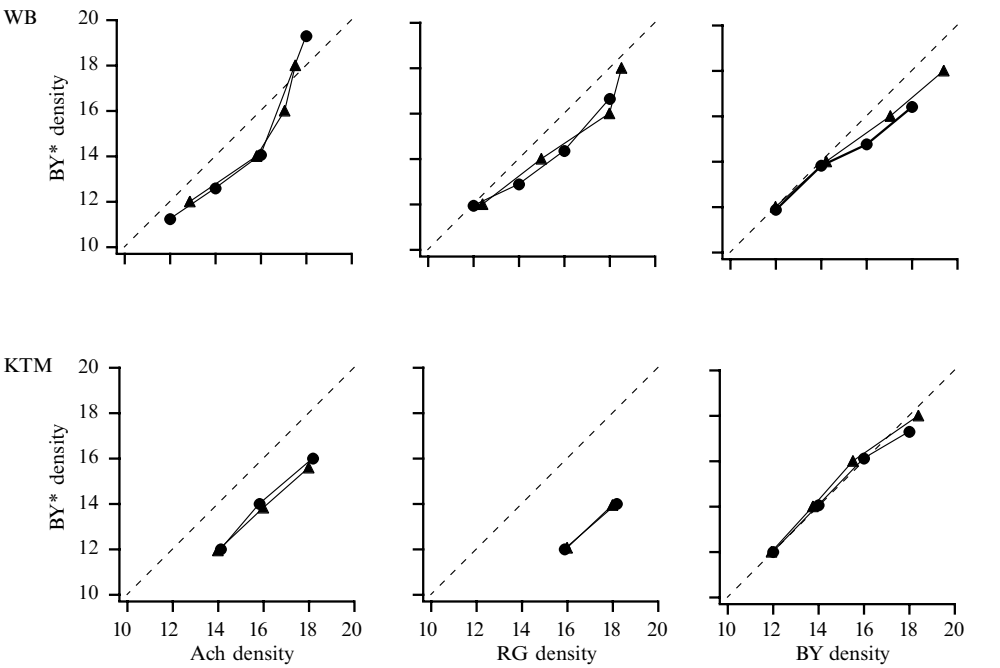

Figure 7. Effect of local orientation cues on density perception. The data points represent perceptual density equivalence for the comparison of the BY stimulus corrected in terms of its local orientation cues with uncorrected Ach, RG, and BY stimuli. In each graph, the vertical axis refers to the corrected BY stimulus (marked with an $*$) while the horizontal axis refers to the uncorrected stimulus. 15 and 20 trials per condition for subjects KTM and WB, respectively. Symbols and dashes are as for figure 2.

Last, we combined the eccentricity-dependent contrast correction and the minimisation of local orientation cues of the BY stimuli for the comparison with the RG stimuli (figure 8). Again, both subjects still show a significant density bias towards the BY stimuli, comparable to the density bias produced by the two types of correction alone (figure 6 and middle panels in figure 7). In conclusion, neither the eccentricity-dependent contrast sensitivity of the RG stimuli nor the presence of local structures can explain the enhancement of perceived density that we report for BY stimuli.

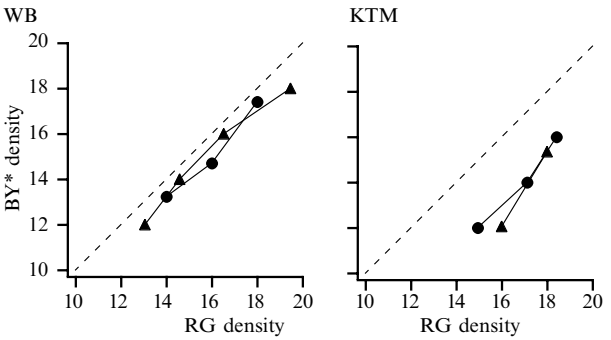

Figure 8. Combined effect of eccentricity and local-orientation cues. The data points represent perceptual density equivalence for the comparison of the BY stimulus corrected in both eccentricity and local-orientation cues with the RG stimuli. 15 and 20 trials per condition for subjects KTM and WB, respectively. Symbols and dashes are as for figure 2.

4 Discussion

We have demonstrated the presence of a singular effect in density perception affecting the blue–yellow cone opponent mechanism: blue–yellow stimuli are perceived as more dense than achromatic and red–green stimuli, despite corrections of factors that might have affected the density perception of blue–yellow stimuli, such as perceived contrast differences, the eccentricity dependence of contrast sensitivity, and the presence of local-orientation cues. Furthermore, the significant increase in perceived density for the blue–yellow mechanism is a global effect arising from the integration of arrays of elements since it is not associated with any increase in the perceived size or spreading of individual blue–yellow elements. The effect is associated with an overall loss of distinctness of the blue–yellow elements which appear to 'melt' into the array, resulting in a greater perceived crowding in comparison to the red–green and achromatic stimuli which remain visually distinct.

4.1 *Origin of the blue–yellow density illusion*

The effect appears to be associated with the poor border distinctness reported for S-cone signals (Tansley and Boynton 1976, 1978; Tansley and Valberg 1979), for which the term 'melting' was first used (Boynton and Greenspon 1972). These studies, however, covered only single chromatic borders, whereas we find that the 'melting' effect is greatly enhanced for element arrays. What causes the effect? First, because our stimuli are all spatially narrow-band and compared at the same spatial frequency, we can rule out any effect of the overall differences in the contrast-sensitivity functions and acuities of the three post-receptoral mechanisms: at a single spatial frequency, differences in the contrast-sensitivity functions of the three mechanisms will only affect the suprathreshold contrast of the elements, and this has already been corrected. Instead, our results imply other intrinsic differences between the spatial processing of the blue–yellow mechanism in comparison with the other two. One possibility lies in the filtering mechanisms used to extract and link the edges from the visual scene. Evidence suggests that red–green colour vision has bandpass filters underlying its overall low-pass contrast-sensitivity envelope that are almost identical in bandwidth to the luminance filters (Losada and Mullen 1994, 1995; Switkes et al 1988). Less is known about spatial filtering by the blue–yellow system, but adaptation experiments suggest it is subserved by two bandpass filters centred on relatively low spatial frequencies and one low-pass filter (Humanski and Wilson 1993). Furthermore, the blue–yellow system has a much sparser sampling of retinal neurons across visual space (Calkins et al 1998; Curcio et al 1991; Dacey and Lee 1994), and is thought to be a part of the third geniculocortical pathway in primates, the konio-cellular pathway, which also

provides sparse inputs to the visual cortex (Ding and Casagrande 1997; Martin et al 1997). These two factors—fewer bandpass spatial filters and poorer spatial sampling—may lead to a degraded spatial representation of the elements and increases in their spatial uncertainty, possibly resulting in the visual effects that we have described. Such an incomplete neural representation might then be compensated by synergistic interactions among blue–yellow cortical cells through intracortical excitatory long-range connections. This may be also reflected in the increase in spatial 'occupancy' of the blue–yellow system, described in the next section.

There are many reports of 'colour spreading' in the literature, but these are mostly not related to the phenomenon that we report here. 'Neon colour spreading' occurs when an illusory colour fills in an area that is demarcated by illusory contours, producing the effect of a transparent surface at a different depth from the generating contours (Bressan et al 1997). It is clearly different from the effect we describe, and, furthermore, occurs for all colours including the achromatic ones. Colour spreading has also been used to describe assimilation effects such as the von Bezold effect and White's effect in which the appearance of one colour is modified by the adjacent colours. Again, this type of 'spreading' applies to all colours and is not specific to the blue–yellow mechanism.

4.2 *Models of density perception*

Several models have been proposed to explain the perception of numerosity (Allik and Tuulmets 1991; van Oeffelen and Vos 1983). According to these studies, an area 'filled' by the elements is the main limiting factor in numerosity perception (Vos et al 1988). To explain this effect, van Oeffelen and Vos (1983) have proposed the CODE algorithm, which determines the contours of the area by a clustering approach based on the relative proximity between neighbouring items. This model is able to predict the sign or direction of many known numerosity illusions (Vos et al 1988), but not their magnitude (Allik and Tuulmets 1991). To model the dependence of perceived numerosity on the spatial configuration of dots, Allik and Tuulmets (1991) have proposed the occupancy model. The basic idea is that the influence of each item is spread over an area much wider than its physical location. While the CODE model assumes that this spread function depends on the distance between each item and its nearest neighbour, the occupancy model simply assumes that the spread function is constant and independent of the spatial proximity of the surrounding items. According to the occupancy model, each dot (element) occupies a circular 'territory' (with a constant radius R), the impact of this 'territory' upon its neighbourhood being reduced by the overlap of neighbouring dots (see figure A1a in the Appendix). The percept of relative numerosity is then predicted from the sum of all the territories (occupancy index), taking into account the overlap: the stimulus with the larger occupancy value is chosen as more numerous.

Our data per se neither support nor contradict the occupancy model of perceived numerosity. However, in view of our result that BY stimuli are perceived as more dense than RG and Ach stimuli, the occupancy model provides several predictions: (i) the blue–yellow Gabor patches should have a larger occupancy radius than the red–green and achromatic elements, which could be reflected in the perceived colour melting of the blue–yellow signal; (ii) there should be a compression of density perception once there is significant overlap of the element territories, and this should be reflected in a loss of sensitivity to density change or in the inability to discriminate changes for large densities; (iii) the compression for BY stimuli should occur before that for RG or Ach stimuli.

We applied the occupancy model to the particular configuration of our stimuli and fitted it to the data to predict the different radii of 'occupancy' for the BY, RG, and luminance post-receptoral mechanisms (see Appendix for details). Table A1 in the Appendix summarises the results of the fitting procedure, and provides estimates of the

occupancy radius for each post-receptoral mechanism. The occupancy model fits our data quite well (figure 9). We found an increase of 81% for the radii of the BY elements and 32% for the radii of the RG elements, relative to the radius of the Ach elements:

$$r_{\mathrm{Ach}} = 0.674 \text{ deg}, \quad r_{\mathrm{RG}} = 0.89 \pm 0.14 \text{ deg}, \quad r_{\mathrm{BY}} = 1.22 \pm 0.38 \text{ deg},$$

averaged across subjects.

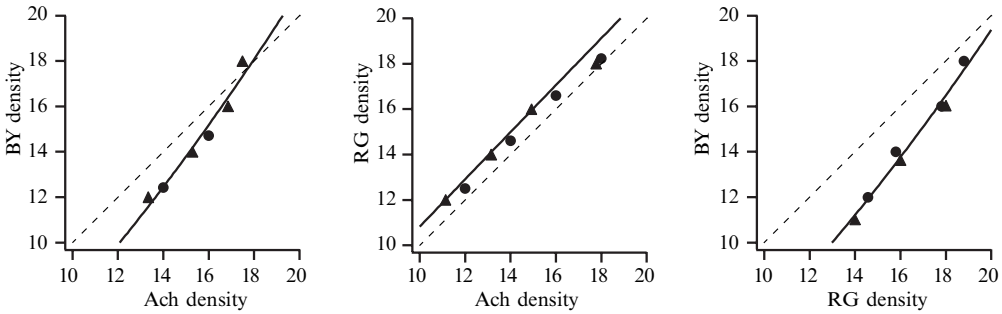

Figure 9. Fit of the occupancy model to the perceptual density equivalence of subject WB. Physical equivalence is represented by the diagonal dashed line. Circle and triangle data points represent the two sets of parameters extracted from the raw data. Thick lines represent fits by the occupancy model (cf Appendix for details).

This result is consistent with the main prediction of the occupancy model: a larger occupancy radius for the BY mechanism accounts very well for its enhanced density perception as well as the spatial spreading of the BY signal between elements. Moreover several plots in figure 2b and figure 3 show a shift of the perceptual isodensity towards the physical isodensity for the higher densities, and sometimes even a crossing (eg subject AR, BY vs RG; subject WB, BY vs Ach). This suggests that the range of four distinguishable densities we considered are close to some limit above which changes in density cannot be detected on the basis of covered area, and that should reflect some saturation in the perception of density [and maybe related to the 'texture-coherence limit' measured by Wilkinson and Wilson (1998)]. A compression at lower densities for the BY mechanism relative to the RG or Ach mechanisms is, however, not evident in our data, but might be revealed if a wider density range were used.

We conclude that difference in the occupancy of each mechanism is the main limiting factor in the perception of density, while other parameters like contrast or local cues affect it only indirectly. The occupancy model may explain some other aspects of our results such as the crossing of the perceptual isodensity curve with the physical isodensity line in the range of densities where the density index is expected to saturate. Finally the larger occupancy radius, melting effect, and density bias of the blue–yellow signal point to spatial processing differences among the post-receptoral mechanisms, which may include differences in their spatial filters, the sparseness of their spatial sampling, and differences in intracortical connectivity.

Acknowledgements. This study was funded by a grant from the Medical Research Council of Canada to K T Mullen (MT-10819) and by a fellowship from the Fyssen Foundation to W H A Beaudot. We acknowledge partial support from the 'Réseau FRSQ de Recherche en Santé de la Vision'. We also thank the subjects who agreed to participate in the study, as well as Anik Rawji for help in collecting data.

References

Alam S, Luccio R, Vardabasso F, 1986 "Regularity, exposure time and perception of numerosity" *Perceptual and Motor Skills* **63**(2 Pt 2) 883 – 888

Allik J, Tuulmets T, 1991 "Occupancy model of perceived numerosity" *Perception & Psychophysics* **49** 303 – 314

Allik J, Tuulmets T, Vos P G, 1991 "Size invariance in visual number discrimination" *Psychological Research* **53** 290 – 295

Anstis S, Cavanagh P, 1983 "A minimum motion technique for judging equiluminance", in *Color Vision: Physiology and Psychophysics* Eds J D Mollon, L T Sharpe (London: Academic Press) pp 155 – 166

Atkinson J, Braddick O, 1992 "Visual segmentation of oriented textures by infants" *Behavioural Brain Research* **49** 123 – 131

Binet A, 1890 "La perception des longeurs et des nombres chez quelques petits enfants" *Revue Philosophique de la France et de l'Étranger* **30** 68 – 81

Bindman D, Chubbs C, 1998 "Visual discrimination of large numerosities" *Investigative Ophthalmology & Visual Science* **39**(4) S859 (abstract 4001)

Boynton R M, 1979 *Human Color Vision* (New York: Holt Rinehart and Winston)

Boynton R M, Greenspon T S, 1972 "The distinctness of borders formed between equally saturated psychologically unique fields" *Vision Research* **12** 495 – 507

Bradley A, Zang L, Thibos L N, 1992 "Failures of isoluminance caused by ocular chromatic aberration" *Applied Optics* **31** 2109 – 2148

Bressan P, Mingolla E, Spillmann L, Watanabe T, 1997 "Neon color spreading: a review" *Perception* **26** 1353 – 1366

Buckley D, Frisby J P, Blake A, 1996 "Does the human visual system implement an ideal observer theory of slant from texture?" *Vision Research* **36** 1163 – 1176

Burgess A, Barlow H B, 1983 "The precision of numerosity discrimination in arrays of random dots" *Vision Research* **23** 811 – 820

Calkins D J, Tsukamoto Y, Sterling P, 1998 "Microcircuitry and mosaic of a blue – yellow ganglion cell in the primate retina" *Journal of Neuroscience* **18** 3373 – 3385

Cole G R, Hine T, 1992 "Computation of cone contrasts for color vision research" *Behavioural Research Methods and Instrumentation* **24** 22 – 27

Cole G R, Hine T, McIlhagga W H, 1993 "Detection mechanisms in L-, M-, and S-cone contrast space" *Journal of the Optical Society of America A* **10** 38 – 51

Cumming B G, Johnston E B, Parker A J, 1993 "Effects of different texture cues on curved surfaces viewed stereoscopically" *Vision Research* **33** 827 – 838

Curcio C A, Allen K A, Sloan K L, Lerea C L, Hurley J B, Klock I B, Milam A H, 1991 "Distribution and morphology of human cone photoreceptors stained with anti-blue opsin" *Journal of Comparative Neurology* **312** 610 – 624

Dacey D M, Lee B B, 1994 "The 'blue-on' opponent pathway in primate retina originates from a distinct bistratified ganglion cell type" *Nature (London)* **367** 731 – 735

Ding Y, Casagrande V A, 1997 "The distribution and morphology of LGN K pathway axons within the layers and CO blobs of owl monkey V1" *Visual Neuroscience* **14** 691 – 704

Durgin F H, Huk A C, 1997 "Texture density aftereffects in the perception of artificial and natural textures" *Vision Research* **37** 3273 – 3282

Ellemberg D, Wilkinson F, Wilson H R, Arsenault A S, 1998 "Apparent contrast and spatial frequency of local texture elements" *Journal of the Optical Society of America A* **15** 1733 – 1739

Field D, Hayes A, Hess R F, 2000 "The roles of polarity and symmetry in the perceptual grouping of contour fragments" *Spatial Vision* **13** 51 – 66

Gibson J, 1950 *The Perception of the Visual World* (Boston, MA: Houghton Mifflin)

Gibson J J, 1979 *The Ecological Approach to Visual Perception* (Hillsdale, NJ: Lawrence Erlbaum Associates)

Ginsburg N, 1976 "Effect of item arrangement on perceived numerosity: randomness vs regularity" *Perceptual and Motor Skills* **43** 663 – 668

Ginsburg N, 1978 "Perceived numerosity, item arrangement, and expectancy" *American Journal of Psychology* **91** 267 – 273

Ginsburg N, 1980 "The regular – random numerosity illusion: rectangular patterns" *Journal of General Psychology* **103** (second half) 211 – 216

Ginsburg N, 1991 "Numerosity estimation as a function of stimulus organization" *Perception* **20** 681 – 686

Ginsburg N, Goldstein S R, 1987 "Measurement of visual cluster" *American Journal of Psychology* **100** 193 – 203
Ginsburg N, Nicholls A, 1988 "Perceived numerosity as a function of item size" *Perceptual and Motor Skills* **67** 656 – 658
Humanski R A, Wilson H R, 1993 "Spatial-frequency adaptation: evidence for a multiple-channel model of short-wavelength-sensitive-cone spatial vision" *Vision Research* **33** 665 – 675
Julesz B, 1981 "A theory of preattentive texture discrimination based on first-order statistics of textons" *Biological Cybernetics* **41** 131 – 138
Julesz B, 1986 "Texton gradients: the texton theory revisited" *Biological Cybernetics* **54** 245 – 251
Kellman P J, Shipley T F, 1991 "A theory of visual interpolation in object perception" *Cognitive Psychology* **23** 141 – 221
Koffka K, 1936 *Principles of Gestalt Psychology* (New York: Harcourt Brace)
Koffka K, Harrower M R, 1931 "Colour and organization" *Psychologische Forschung* **15** 145 – 275
Krueger L, 1972 "Perceived numerosity" *Perception & Psychophysics* **11** 5 – 9
Losada M A, Mullen K T, 1994 "The spatial tuning of chromatic mechanisms identified by simultaneous masking" *Vision Research* **34** 331 – 341
Losada M A, Mullen K T, 1995 "Color and luminance spatial tuning estimated by noise masking in the absence of off-frequency looking" *Journal of the Optical Society of America A* **12** 250 – 260
Martin P R, White A J, Goodchild A K, Wilder H D, Sefton A E, 1997 "Evidence that blue-on cells are part of the third geniculocortical pathway in primates" *European Journal of Neuroscience* **9** 1536 – 1541
McIlhagga W, Hine T, Cole G R, Snyder A W, 1990 "Texture segregation with luminance and chromatic contrast" *Vision Research* **30** 489 – 495
McIlhagga W H, Mullen K T, 1996 "Contour integration with colour and luminance contrast" *Vision Research* **36** 1265 – 1279
Mullen K T, 1991 "Colour vision as a postreceptoral specialization of the central visual field" *Vision Research* **31** 119 – 130
Mullen K T, Kingdom F A, 1996 "Losses in peripheral colour sensitivity predicted from 'hit and miss' post-receptoral cone connections" *Vision Research* **36** 1995 – 2000
Mullen K T, Beaudot W H A, McIlhagga W H, 2000 "Contour integration in color vision: a common process for the blue – yellow, red – green and luminance mechanisms?" *Vision Research* **40** 639 – 655
Mulligan J B, MacLeod D I A, 1988 "Reciprocity between luminance and dot density in the perception of brightness" *Vision Research* **28** 503 – 519
Nawrot M, Shannon E, Rizzo M, 1996 "The relative efficacy of cues for two-dimensional shape perception" *Vision Research* **36** 1141 – 1152
Nothdurft H C, 1985 "Sensitivity for structure gradient in texture discrimination tasks" *Vision Research* **25** 1957 – 1968
Nothdurft H C, 1990 "Texton segregation by associated differences in global and local luminance distribution [erratum in **241** 249-50]" *Proceedings of the Royal Society of London, Series B: Biological Sciences* **239** 295 – 320
Oeffelen M P van, Vos P G, 1983 "An algorithm for pattern description on the level of relative proximity" *Pattern Recognition* **16** 341 – 348
Pollack R H, Brenner M J, 1969 *The Experimental Psychology of Alfred Binet* (New York: Springer)
Sagi D, Julesz B, 1987 "Short-range limitation on detection of feature differences" *Spatial Vision* **2** 39 – 49
Sankeralli M J, Mullen K T, 1996 "Estimation of the L-, M- and S-cone weights of the post-receptoral detection mechanisms" *Journal of the Optical Society of America A* **13** 906 – 915
Sireteanu R, Rieth C, 1992 "Texture segmentation in infants and children" *Behavioural Brain Research* **49** 133 – 139
Smith V C, Pokorny J, 1975 "Spectral sensitivity of the foveal photopigments between 400 and 500 nm" *Vision Research* **15** 161 – 171
Stevens K A, 1981 "The information content of texture gradients" *Biological Cybernetics* **42** 95 – 105
Switkes E, Bradley A, De Valois K K, 1988 "Contrast dependence and mechanisms of masking interactions among chromatic and luminance gratings" *Journal of the Optical Society of America A* **5** 1149 – 1162
Tansley B W, Boynton R M, 1976 "A line, not a space, represents visual distinctness of borders formed by different colors" *Science* **191** 954 – 957
Tansley B W, Boynton R M, 1978 "Chromatic border perception: the role of red- and green-sensitive cones" *Vision Research* **18** 683 – 697

Tansley B W, Valberg A, 1979 "Chromatic border distinctness: not an index of hue or saturation differences" *Journal of the Optical Society of America* **69** 113 – 118
Taves E H, 1941 "Two mechanisms for the perception of visual numerousness" *Archives of Psychology* **37** 1 – 47
Vos P G, Oeffelen M P van, Tibosch H J, Allik J, 1988 "Interaction between area and numerosity" *Psychological Research* **50** 148 – 154
Wilkinson F, Wilson H R, 1998 "Measurement of the texture-coherence limit for bandpass arrays" *Perception* **27** 711 – 728
Williams C B, Hess R F, 1998 "Relationship between facilitation at threshold and suprathreshold contour integration" *Journal of the Optical Society of America A* **15** 2046 – 2051

APPENDIX: Application of the occupancy model

We applied the occupancy model to the specific configuration of our stimuli by taking stimulus size and quasi-regular arrangement of the Gabor patches into account. We assume that the occupancy area of a single Gabor patch is circular. We define the occupancy index as the total area covered by all elements of the stimulus (figure A1). Using geometric considerations, we estimated the occupancy index in nonoverlapping and overlapping configurations as a continuous function of the number of elements.

(a) In a nonoverlapping configuration the distance between the centres of the closest circular areas of radius r is greater or equal to $2r$. The total area covered by the elements

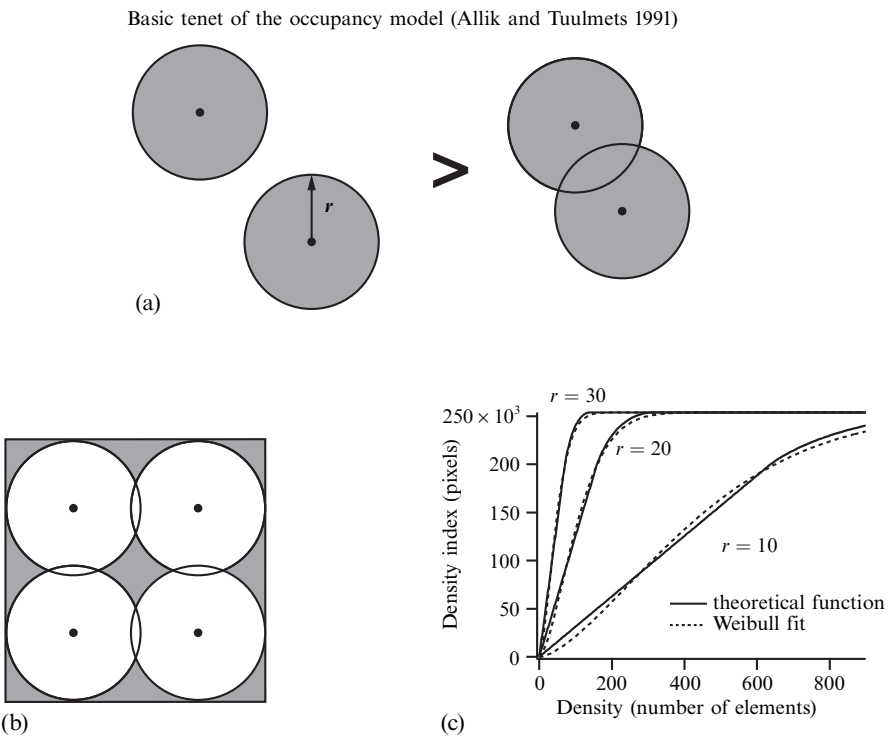

Figure A1. (a) The occupancy model (Allik and Tuulmets 1991): the density index measures the total area covered by the area (of radius r) influenced by the individual elements composing the stimulus. For example, the configuration consisting of nonoverlapping elements (left) has a greater density index than a configuration consisting of overlapping elements (right). (b) The geometrical configuration of the elements considered in the context of the occupancy model: regular arrangement of elements according to a square grid. The grey area represents the part of the visual representation of the stimulus not influenced by any elements. (c) Density index functions derived for the occupancy model. The plain curves are the theoretical model, while the dashed curves are their Weibull fits.

is then $D_i = n^2\pi r^2$ where n is the number of elements per side of the square stimulus (total of n^2 elements). In this configuration, the density index (D_i) is linearly related to the number of elements with a slope depending directly on the occupancy radius r.
(b) An overlap appears when the distance between the centres of the closest circular areas is less than $2r$. The effective density index is then reduced by an amount which depends on the overlap. Rather than estimating directly the covered area, we estimated the non-covered area, $A_{\text{non-covered}}$ (grey area in figure A1b where $n = 2$) and subtracted it from the total area, A_{total}, of the stimulus:

$$D_i = A_{\text{total}} - A_{\text{non-covered}} ,$$

where

$$A_{\text{non-covered}} = 4n^2[R_{\text{opt}}^2 - R_{\text{opt}}(r^2 - R_{\text{opt}}^2)^{1/2} - \tfrac{1}{2}\theta r^2] ,$$

$$R_{\text{opt}} = A_{\text{total}}^{1/2}/2n ,$$

$$\theta = \tfrac{1}{2}\pi - 2\arctan[(r^2 - R_{\text{opt}}^2)^{1/2}/R_{\text{opt}}] .$$

(c) The overlap is maximum when the distance between the centres is less than $r\sqrt{2}$. The density index then reaches a saturation point which corresponds to the total area covered by the stimulus, that is A_{total}.

Figure A1c shows some examples of the density index function for several values of the occupancy radius. The density index increases first linearly with the density in non-overlapping configurations, then is compressed when the elements begin to overlap before saturating for full overlap.

This occupancy index function has a sigmodal shape, and can be approximated for example by a Weibull function:

$$D_i^* = A_{\text{total}}\{1 - \exp[-(x/\alpha)^{\beta}]\} ,$$

where $x = n^2$. Within this approximation, α is inversely proportional to r^2 (the relation $\alpha = \text{constant}/r^2$ holds over a wide range of parameters), and β is roughly constant (≈ 1.58).

Two stimuli with different physical densities appear as equally dense when their density indexes are equal, that is $D_{i1}^* = D_{i2}^*$ when the Weibull fit is used. This perceptual isodensity line is described by the function:

$$x_1 = \alpha_1 \left(\frac{x_2}{\alpha_2}\right)^{\beta_2/\beta_1} .$$

If $\beta_2 \neq \beta_1$, this perceptual isodensity line crosses the physical isodensity line for a density given by:

$$\alpha = \left(\frac{\alpha_2^{\beta_2}}{\alpha_1^{\beta_1}}\right)^{1/(\beta_2 - \beta_1)} .$$

We fitted this isodensity function to the data of figures 2b and 3 for all subjects (results shown only for subject WB in figure 9), and derived an estimation of the occupancy radius for each post-receptoral mechanism. However, this fitting procedure can only provide assessment to relative radii, so we have to consider reference radii for one of the mechanisms. Mulligan and MacLeod (1988) have shown that element brightness increases with luminance dot density, and suggested that brightness is integrated over a distance of about 30 min of arc in radius. Allik and Tuulmets (1991) provided an estimate of about 20 min of arc for the occupancy radius in perception of dot density. Since the elements composing our stimuli are much larger than dots, the occupancy radius for the achromatic elements is likely to be larger than these estimates but probably not very much larger than the occupancy area covered by all pixels contained in one

space constant (0.17 deg or 10 min of arc) of the Gabor element. We assumed that the occupancy radius of the achromatic element is approximately equal to 40 min of arc, and we constrained the set of free parameters by setting α and β parameters of the achromatic mechanism to values derived from the Weibull fit of its theoretical density index function ($\alpha = 84.27$ and $\beta = 1.5822$, cf figure A1c).

We first fitted the model to the BY vs Ach data to estimate parameters for the blue–yellow mechanism, then using these estimates we fitted the model to the BY vs RG data to obtain parameters for the red–green mechanism. Table A1 summarises the results of the fitting procedure and the resulting estimation of the occupancy radius for each mechanism and each subject. The fits are represented by plain lines in figure 9: for the RG vs Ach data (middle panel) the plain line represents the prediction of the model when considering the estimation of parameters for the BY vs Ach data (left panel) and BY vs RG data (right panel). The data are generally better fitted with different values of the β parameter compared to the fit of the theoretical density index ($\beta \approx 1.58$), which suggests that other factors may affect the density perception by modifying the slope of the density index function. An intrinsic difference between the post-receptoral mechanisms could possibly account for this difference.

Table A1. Occupancy radius for each post-receptoral mechanism derived by fitting the occupancy model to the data shown in figures 2b and 3: α and β are the parameters of the Weibull function used to approximate the theoretical density index function, while r is an estimate of the occupancy radius given in degree of visual angle.

Subject	Ach			RG	BY				
	α	β	r	α	β	r	α	β	r
KTM				45.955	1.0207	0.91	10.142	0.64145	1.94
WB				99.098	1.6321	0.62	44.269	1.0656	0.93
AR	84.27	1.5822	0.674	40.728	1.0834	0.97	24.996	0.91357	1.24
JL				43.264	0.94396	0.94	38.785	1.2372	0.99
JM				36.791	1.8117	1.02	39.098	2.0915	0.99